Author Manuscript

Author Manuscript

Author Manuscript

Author Manuscript

HHS Public Access

Author manuscript

Immunohorizons. Author manuscript; available in PMC 2019 September 11.

Published in final edited form as:

Immunohorizons. ; 3(8): 389–401. doi:10.4049/immunohorizons.1900030.

Antigen Complexed with a TLR9 Agonist Bolsters c-Myc and mTORC1 Activity in Germinal Center B Lymphocytes

Eric J. Wigton[*,†], **Anthony L. DeFranco**[†], **K. Mark Ansel**[*,†]

[*]Sandler Asthma Basic Research Center, University of California, San Francisco, San Francisco, CA 94143;

[†]Department of Microbiology and Immunology, University of California, San Francisco, San Francisco, CA 94143

Abstract

The germinal center (GC) is the anatomical site where humoral immunity evolves. B cells undergo cycles of proliferation and selection to produce high-affinity Abs against Ag. Direct linkage of a TLR9 agonist (CpG) to a T-dependent Ag increases the number of GC B cells. We used a T-dependent Ag complexed with CpG and a genetic model for ablating the TLR9 signaling adaptor molecule MyD88 specifically in B cells (B-MyD88^{-} mice) together with transcriptomics to determine how this innate pathway positively regulates the GC. GC B cells from complex Ag-immunized B-MyD88^{-} mice were defective in inducing gene expression signatures downstream of c-Myc and mTORC1. In agreement with the latter gene signature, ribosomal protein S6 phosphorylation was increased in GC B cells from wild-type mice compared with B-MyD88^{-} mice. However, GC B cell expression of a c-Myc protein reporter was enhanced by CpG attached to Ag in both wild-type and B-MyD88^{-} mice, indicating a B cell–extrinsic effect on c-Myc protein expression combined with a B cell–intrinsic enhancement of gene expression downstream of c-Myc. Both mTORC1 activity and c-Myc are directly induced by T cell help, indicating that TLR9 signaling in GC B cells either enhances their access to T cell help or directly influences these pathways to further enhance the effect of T cell help. Taken together, these findings indicate that TLR9 signaling in the GC could provide a surrogate prosurvival stimulus, “TLR help,” thus lowering the threshold for selection and increasing the magnitude of the GC response. *ImmunoHorizons*, 2019, 3: 389–401.

This article is distributed under the terms of the CCBY-NC4.0Unported license

Address correspondence and reprint requests to: Dr. Anthony L. DeFranco or Dr. K. Mark Ansel, Department of Microbiology and Immunology, University of California, San Francisco, 513 Parnassus Avenue, University of California, San Francisco Box 0414, San Francisco, CA 94143 (A.L.D.) or Sandler Asthma Basic Research Center, University of California, San Francisco, 513 Parnassus Avenue, University of California, San Francisco Box 0414, San Francisco, CA 94143 (K.M.A.). Anthony.defranco@ucsf.edu (A.L.D.) or mark.ansel@ucsf.edu (K.M.A.).

E.J.W., K.M.A., and A.L.D. conceived of experiments, analyzed/interpreted data, and wrote the manuscript. E.J.W. conducted all the experiments and generated all figures.

DISCLOSURES

The authors have no financial conflicts of interest.

The sequences presented in this article have been submitted to the Gene Expression Omnibus (https://www.ncbi.nlm.nih.gov/geo/query/acc.cgi?acc=GSE126849) under accession number GSE126849.

The online version of this article contains supplemental material.

Author Manuscript Author Manuscript Author Manuscript Author Manuscript

TLRs recognize pathogen-associated molecular patterns and serve as key mediators of the innate immune response against pathogens. However, TLRs are expressed on both adaptive and innate immune cells. Deficiency in these receptors or their key signaling molecules, such as MyD88, impairs both innate and adaptive responses to pathogens (1–3). The dual function of TLRs in initiating the early inflammatory response while at the same time directly shaping the slower Ag-specific adaptive response shows that these receptors act through multiple elements within the immune system. It has been appreciated for a number of years that several TLRs are expressed by B cells, and these receptors regulate B cell activation and fate decisions (4, 5). Studies using mice in which the critical TLR signaling component MyD88 is selectively ablated in B cells or mixed bone marrow chimeras in which B cells were selectively deficient in a particular TLR revealed that such mice also have substantial defects in germinal center (GC) and plasma cell generation and in isotype-switched Ab titers in response to multiple TLR agonists mixed with T-dependent and T-independent Ags (6–8).

This biological role for TLR signaling in B cells is important for making high-quality Abs to a number of viral infections of mice, in which case endosomal TLR7 and TLR9, which recognize nucleic acids, are critical (6, 9). BCR-mediated endocytosis of the Ag and associated BCR signaling delivers TLR ligands to the endosomal location of these receptors (10, 11). In addition, TLR7 and TLR9 function in B cells is required for the production of anti-DNA and antiribonucleoprotein autoantibodies in several mouse models of systemic lupus erythematosus (12).

One experimental strategy for studying how BCR signaling and TLR9 signaling enhance the GC response is to immunize with a T-dependent Ag physically coupled to a synthetic TLR9 agonist, CpG deoxyoligonucleotide (oligo) (13). To activate the potential of TLR9 to enhance a GC response, the Ag must be oligovalent (as is the case for a haptenated protein) (13). The TLR9 ligand can be present in virus-like particles (VLPs) (7, 14) or combined with DOTAP adjuvants (15) to form liposome-like oligovalent Ags. MyD88 deficiency in B cells compromises GC B cell numbers and Ab titers to such Ags (7, 13), but how TLR signaling enhances the response that remains dependent upon T follicular helper (Tfh) cells is unclear. In a murine model of autoimmune lupus in which TLR7 and TLR9 are necessary for sustained autoreactive B cell responses, cognate autoreactive T cells could partially rescue GC B cell activation defects in the absence of TLR7/9 (16). This suggests the overlap of prosurvival signals derived from T cell help and TLR7/9 signaling in supporting GC B cell survival and humoral immunity, but the molecular nature of the signals provided by TLRs was not defined.

In this study, we explored the mechanistic basis by which a TLR9 ligand attached to an Ag signals within the Ag-specific B cell to promote the GC response. The wild-type (WT) GC B cells immunized with 4-hydroxy-3-nitro-phenylacetyl (NP)–haptenated T-dependent Ag complexed with a CpG oligo had increased oxidative phosphorylation, mTORC1, and c-Myc gene expression signatures compared with MyD88-deficient GC B cells. Remarkably, both c-Myc and mTORC1 are induced by Tfh cell–mediated interactions with GC B cells through CD40L:CD40 signaling (17–19). As such, MyD88-dependent TLR9 signaling induced gene expression signatures that were previously associated with Tfh cell help, suggesting that

Author Manuscript Author Manuscript Author Manuscript Author Manuscript

TLR signaling in GC B cells enhanced the GC response by mimicking the effects of Tfh on the B cells, without replacing the requirement for Tfh. Together, these findings indicate that TLR9 signaling in GC B cells can provide a supplemental stimulus that allows more B cells to occupy the GC in an environment where Tfh cell help is limiting for survival.

MATERIALS AND METHODS

Generation of complex Ags and BCR stimulants

NP–chicken γ globulin (CGG) complex Ag was generated similarly to what has been previously published, with the following modi-fications:NP(14–30)CGG(Biosearch) was biotinylated using biotin(xx)-NHSS in DMF, as previously reported (13). The biotinylated NP(14–30)CGG was mixed (5 mg/ml) with streptavidin (Thermo Fisher Scientific) (10 mg/ml) and 5’ biotinylated CpG oligo 1826 (5’-CCATGACGTTCCTGACGTT-3’) (IDT) or a 5’ biotinylated non-CpGoligo(5’-TCCAGGACTTCTCTCAGGTT-3’)(IDT)(5mg/ml) at a molar ratio of 1:4:48, respectively, in PBS for 24 h before being washed in 5 ml of PBS in an Amicon Ultra-15 Centrifugal Filter Unit 10 kD (Millipore) three times and resuspended at 100 μg of total mass per 50 μl. Similarly, biotinylated anti-IgM (goat polyclonal; Jackson ImmunoResearch) was mixed with streptavidin and 5’ biotinylated CpG oligo 1826 (IDT) or a 5’ biotinylated non-CpG oligo (5 mg/ml) at a molar ratio of 2:1:2 in PBS for 24 h before being transferred to an Amicon Ultra-15 Centrifugal Filter Unit 10 kD filter (Millipore), washed three times with PBS, and resuspended at 1.5 μg anti-IgM per microliter.

Mice and immunizations

Mice used in these experiments consisted of Mb1-cre [C(Cg)-Cd79a$^{tm1(cre)Reth}$/EhobJ], MyD88flox[B6.129P2(SJL)-MyD88^{tm1Defr}/J], c-Myc-GFP reporter (B6;129-Myc^{tm1Slek}/J) (backcrossed 10 timestoB6/J), and Em-Bcl2transgenic[C.Cg-Tg(BCL2)22Wehi/J] (a gift from the Cyster laboratory), all of which were maintained in house, according to all Institutional Animal Care and Use Committee guidelines.

Mice were immunized s.c. in the scruff and flanks with a total of 100 μg of NP-CGG in complex Ag for cell sorting and in vivo phospho-flow experiments and with 25 μg of NP-CGG complex Ag in the footpad for c-Myc-GFP and general flow cytometry experiments. Draining lymph nodes were analyzed. Em-BCL2 transgenic c-Myc-GFP mice were immunized with 100 μg of NP (14–30)-CGG (Biosearch) in Alum Imject (Thermo Fisher Scientific)i.p., and GC B cells were isolated from spleen 12–14 d later.

RNA isolation and mRNA sequencing

Ten thousand NP^{+} GC B cells were collected by FACS sorting directly into the lysis buffer of the Dynabead direct mRNA extraction kit (Thermo Fisher Scientific). mRNA was isolated by use of poly-dT beads, according to the manufacturer’s instructions (Thermo Fisher Scientific). Library preparation and RNA sequencing (RNA-seq) was performed through the University of California, San Francisco Functional Genomics Core, aligned to the Ensembl mouse GRCh38.78 (mm10) genome using STAR software, and analyzed using DESeq2, as previously reported (20).

Author Manuscript Author Manuscript Author Manuscript Author Manuscript

Flow cytometry

Single-cell suspensions were prepared from draining lymph nodes or spleen by gently passing them through 70-μm nylon mesh filters. Cells were collected by centrifugation and incubated with anti-CD16/CD32 (2.4G2) in FACS buffer (PBS + 2% FBS + 2 μm EDTA + 0.01% NaN_3) to block Ab binding to Fc receptors before staining with Abs for surface markers. For phospho-flow analysis of in vivo cells, mice were perfused with 10% paraformaldehyde directly after sacrifice (Sigma-Aldrich), and single-cell suspensions from lymph nodes were prepared directly in 2% paraformaldehyde and incubated for 15 min on ice before permeabilizing the cell plasma membranes with ice-cold methanol. Fixed cells were rehydrated with PBS, washed by centrifugation in FACS buffer, and blocked and stained with Abs, as described above. Conjugated Abs used included PE-Cy7 anti-CD95 (Jo2), FITC and PerCP-Cy5.5 anti-GL7, BV605 anti-CD19 (6D5), FITC anti-B220 (RA3–6B2), biotin anti-CD11c, biotin anti-CD3e (145–2C11), biotin anti-Ter119, biotinanti-Gr1, ef450 anti-IgD (11–26c), biotin anti-CXCR4(2B11), APC anti-CD86 (GL-1), APC anti-CD83 (Michel-19), AF647 anti-pS6(ser240/244) (D68F8), AF647 anti-pS6(ser235/236) (D57.2.2E), and AF647 anti-pAkt ser473 (D9E). Biotin conjugates were detected using BV711 or BV786 streptavidin (BioLegend). NP (8–30)-PE (Biosearch) was used to detect NP-binding B cells. Dead cells were detected using efluor780 or UV blue fixable viability dyes (Thermo Fisher Scientific). Flow cytometry analysis and sorting were performed on LSR II and FACSAria II cytometers (BD Biosciences), respectively.

In vitro and ex vivo naive and GC B cell isolation and stimulation

WT, Mb1-cre^{+} MyD88$^{fl/fl}$ (B-MyD88^{-}), WT-c-Myc-GFP, and Mb1-cre^{+} MyD88$^{fl/fl}$Myc-GFP$^{+/+}$(B-MYD88^{-} c-Myc-GFP)naive B cells were isolated using Dynabead negative CD43 selection kit (Thermo Fisher Scientific) and stimulated in RPMI 1640 supplemented with 10% FCS, HEPES, 2-ME, and L-glutamine with anti–IgM-CpG and anti–IgM-Non for 24 h, then stained for viability before being analyzed by flow cytometry or fixed before staining for phospho-flow. Eμ-BCL2 Myc-GFP B cells were isolated by anti-CD11c, anti-CD43, and anti-IgD (GC) or anti-GL7 (naive) biotin Abs, followed by an antibiotin magnetic bead isolation (Miltenyi), according to a previously published protocol (21). Purity was confirmed at least 95% B220^{+} for naive B cells and 90% Fas^{+}, CD38^{2} for GC B cells. Cells were stimulated with 10–20 μg of anti-CD40 (FGK4.51; Miltenyi), 10–20 μg of anti-IgM (goat polyclonal μ chain; Jackson ImmunoResearch), 75 nM CpG 1826 oligo (IDT), or combinations of these reagents for 4 h in complete RPMI 1640 medium and processed for flow cytometry.

Software and statistics

Data visualization and statistical calculations were performed using Prism (GraphPad). Statistical tests and *p* values for each experiment are specified in figure legends. For a single comparison between two groups, a Student *t* test was used; for multiple comparisons between preselected groups, a one-way ANOVA test with Holm–Sidak correction for multiple comparisons was used; and for multiple comparisons in which all groups were compared, a one way ANOVA test with a Tukey correction for multiple comparisons was used. Flow cytometry data were analyzed with FlowJo.

Author Manuscript Author Manuscript Author Manuscript Author Manuscript

Gene Set Enrichment Analysis (GSEA) was run on the graphical user interface according to the manufacturer's recommendations (https://software.broadinstitute.org/gsea/doc/GSEAUserGuideFrame. html) to compare the WT and MyD88^{-} RNA-seq data sets using all genes (22).

RNA-seq data are publicly available on the Gene Expression Omnibus under accession number GSE126849 (https://www.ncbi.nlm.nih.gov/geo/query/acc.cgi?acc=GSE126849.

RESULTS

TLR9 agonist complexed to T-dependent Ag increases the frequency and number of GC B cells in responseto immunization

Previous studies have demonstrated that attachment of a TLR7 or TLR9 ligand to an Ag can boost the GC Ab response (7, 13). We created two complex Ags composed of biotinylated NP-CGG complexed with streptavidin and either biotinylated CpG oligo or biotinylated control oligo yielding NP-CGG-CpG or NP-CGG-Non, respectively (13). C57BL/6 mice were immunized s.c. with either NP-CGG-CpG or NP-CGG-Non, and the GC response was analyzed at day 14 (D14) (Supplemental Fig. 1A). As the high-affinity anti-NP Ab response to NP-CGG is known to have a substantial contribution of λ L chain–containing Abs, we also analyzed the frequency of NP-binding, λ^{+} GC B cells. Mice immunized with NP-CGG-CpG showed a 3.5-fold increase in the number of total GC B cells (CD19^{+}, IgD^{lo}, Fas^{+}) as well as a 4-fold increase in the number of NP-binding λ^{+} GCB cells (Supplemental Fig.1B, 1C). These results agree with a previous study using a similar complex Ag (13).

To specifically test the role of TLR9 agonism in the B cell compartment, we immunized B cell lineage-specific MyD88-deficient (B-MyD88^{-}) and control Mb1-cre^{+} MyD88$^{fl/+}$ or Mb1-cre^{+} MyD88$^{+/+}$ (WT) mice with NP-CGG-CpG Ag and analyzed the GC response at D14 (Supplemental Fig. 1D, 1E). WT mice exhibited a 2.4-fold higher frequency and number of GL7^{hi} GC B cells as compared with the B-MYD88^{-} mice (Fig. 1A). Thus, in agreement with previous work, these results show that B cell TLR9 signaling enhances the GC response to a haptenated Ag attached to a TLR9 ligand. There was also likely to be some contribution of TLR signaling in another cell type, such as classical dendritic cells.

NP-CGG-CpG Ag induces MyD88-dependent c-Myc and mTORC1 signature gene expression

To determine the effect of TLR9 signaling on the GC response at a transcriptional level, we performed mRNA sequencing on NP-binding WT and B-MYD88^{-} GC B cells at D14 postimmunization with NP-CGG-CpG, using the gating strategy illustrated in Supplemental Fig. 1E. This analysis uncovered 479 differentially expressed genes (false discovery rate [FDR] < 0.05 by Fisher exact test), of which 260 were increased in WT and 219 were increased in B-MYD88^{-} cells. Among the genes with higher expression in WT GC B cells, many corresponded to ribosomal proteins, NADH dehydrogenase, ATP synthase, and cytochrome oxidase machinery, pointing toward increased oxidative phosphorylation activity (Fig. 1B). This metabolic phenotype is consistent with the recent finding that TLR9 signaling can rescue naive B cells from apoptosis resulting from mitochondrial dysfunction

Author Manuscript Author Manuscript Author Manuscript Author Manuscript

elicited by BCR engagement in the absence of CD40 or TLR signals (23). There was also increased *Ighg2c* gene expression in WT samples compared with B-MYD88^{-} samples as well as increased expression of *Aicda*, the gene encoding the activation-induced cytidine deaminase that is directly involved in somatic hypermutation and in class-switch recombination (Table I). These results are consistent with the strong effect of the TLR9 ligand in promoting class switch to IgG2a/IgG2c (8, 13). Surprisingly, expression of the transcriptional regulator Bcl6, which directs the GC fate in B cells, was increased in B-MYD88^{-} GC B cells (Table I). Conversely, mRNA encoding the survival factor Bcl2 was higher in WT cells (Table I), suggesting that increased survival may contribute to the increased GC B cell frequency and number in the context of intact TLR9/MyD88 signaling.

To gain greater insight from the mRNA expression data sets, we applied GSEA to the hallmark gene sets (22). Gene sets enriched in WT compared with B-MYD88^{-} GC B cells included the Myc signature with a normalized enrichment score (NES) = 2.38 and FDR < 10^{-5}, the E2F signature with an NES = 1.60 and FDR = 0.02, and the mTORC1 signature with an NES = 1.46 and FDR = 0.057 (Fig. 3B, Table II). We performed a leading-edge analysis on the hallmark subsets from Table II and found that the genes driving the difference in the context of mTORC1 and c-Myc had very little overlap, and thus these two gene signatures represented independent enrichments (Supplemental Fig. 2). Similarly, independently curated mTORC1 (24) and c-Myc (25) gene sets were also enriched in WT compared with B-MYD88^{-} GC B cells (Fig. 1D, 1E, Table II). Furthermore, the KEGG ribosomal pathway showed a large enrichment in WT GC B cells (Table II). From our RNA-seq, *Aicda* was increased 2-fold in WT compared with B-MYD88^{-} cells (FDR = 0.088), concordant with this being positively regulated by mTORC1 signaling (26, 27). In contrast, no hallmark gene sets were enriched in the Ag-specific B-MYD88^{-} GC B cells compared with the Ag-specific WT GC B cells (FDR q values.0.25, data not shown). Interestingly, both c-Myc and mTORC1 have been implicated as downstream effectors of Tfh cell help and their dysregulation negatively impacts the GC response (17–19). These results suggest that TLR9-MyD88 signaling in the Ag-specific GC B cell increases the transcriptional outputs of the c-Myc and mTORC1 pathways, either via direct transcriptional effects or indirectly by enhancing the ability of the GC B cells to interact with Tfh cells and receive CD40L and cytokine signals, which are known to promote these two programs.

TLR9 signaling in naive B cells increases c-Myc expression

To better understand how TLR9 signaling enhances the c-Myc pathway transcriptional response, we examined the effect of BCR signaling and TLR9 signaling on c-Myc protein expression. First, naive polyclonal B cells were stimulated through the BCR and TLR9 in a linked fashion by the addition of anti-IgM bound to streptavidin and biotin-conjugated CpG or biotinylated control oligos to make the complex artificial Ags anti–IgM-CpG and anti–IgM-Non, respectively (28). To measure the c-Myc protein expression on a single-cell level, we crossed a knock-in c-Myc-GFP protein fusion reporter (29) to WT and B-MYD88^{-} mouse strains. We stimulated purified naive B-MYD88^{-} Myc-GFP or WT Mb1-cre^{+}, MyD88$^{+/+}$ c-Myc-GFP$^{+/+}$ (WT-Myc-GFP) splenic B cells with either anti–IgM-CpG or anti–IgM-Non for 24 h and then analyzed the cells for c-Myc-GFP expression by flow cytometry (Fig. 2A). The presence of a TLR9 ligand attached to the anti-IgM Abs greatly

Author Manuscript Author Manuscript Author Manuscript Author Manuscript

enhanced c-Myc expression in naive B cells after 24 h, at which time, 90% of WT-Myc-GFP cells stimulated with anti–IgM-CpG were c-Myc-GFP$^+$ (Fig. 2B). In contrast, WT-Myc-GFP cells stimulated with anti–IgM-Non and B-MyD88$^-$Myc-GFP cells stimulated with either anti–IgMCpG or anti–IgM-Non exhibited much lower c-Myc induction at this time, with 5–10% c-Myc-GFP$^+$ cells (Fig. 2B). Less than 2% of unstimulated naive B cells of either genotype were c-Myc-GFP$^+$. Per cell, c-Myc-GFP abundance was also increased by TLR9/MyD88 signaling, with anti–IgM-CpG–stimulated WT-Myc-GFP B cells displaying a 4-fold increase in GFP mean fluorescence intensity (MFI) compared with anti–IgM-Non–stimulated WT-Myc-GFP and B-MyD88$^-$Myc-GFP cells under either stimulation condition (Fig. 2B). Thus, in naive B cells, combined Ag receptor and TLR9 signals induced c-Myc levels much more strongly than Ag receptor signals alone.

Attachment of a TLR9 ligand to the Ag increased the frequency of GC B cells expressing c-Myc protein in a non–cell-intrinsic manner

We next used the c-Myc-GFP reporter to address the mechanism by which attachment of a TLR ligand to CGG increased the c-Myc transcriptional signature in GC B cells. Previous work established that CD40L delivered by Tfh cells strongly induces c-Myc expression in light zone (LZ) GC B cells, which consequently return to the dark zone (DZ) and undergo further clonal expansion (17, 18). Therefore, we examined c-Myc-GFP expression in D14 LZ and DZ phenotype GC B cells, identified by elevated CD86/CD83 or CXCR4 expression, respectively, from c-Myc-GFP$^{+/+}$ mice immunized with NP-CGG-CpG or NP-CGG-Non Ag (Fig. 2C, Supplemental Fig. 3A) (30, 31). Both immunization groups had similar distributions of DZ and LZ phenotype cells among GC B cells (NP-CGG-CpG: DZ = 51 ± 6%, LZ = 41 ± 5%; NP-CGG-Non: DZ = 52 ± 10%, LZ = 44 ± 9%) (Supplemental Fig. 3A). In agreement with our sequencing data, the NP-CGG-CpG Ag group had a higher percentage (2.7% versus 1.1%) and a greater mean number (3000 versus 1700) of c-Myc-GFP$^+$ GC B cells than NP-CGG-Non–immunized animals (Fig. 2D). A majority of c-Myc-GFP$^+$ cells exhibited an LZ phenotype for both immunization conditions (NP-CGG-CpG: 66 ± 9%; NP-CGG-Non: 69.8 ± 13%)(Supplemental Fig. 3B), consistent with previous studies showing enrichment of the LZ phenotype(31) and localization of c-Myc$^+$ GC B cells to the LZ (17, 18).

To test whether TLR9/MyD88 signaling in the GC B cells contributed to the increased frequency of c-Myc–expressing GC B cells seen upon immunization with NP-CGG-CpG, we immunized WT-Myc-GFP and B-MyD88$^-$Myc-GFP mice with either one allele or two alleles of the c-Myc-GFP fusion reporter and analyzed c-Myc-GFP expression at D14. Interestingly, neither the number nor percentage of c-Myc-GFP$^+$ GC B cells was increased in the GC B cells from WT-Myc-GFP mice compared with the GC B cells from the B-MyD88$^-$ Myc-GFP mice (Fig. 2E). The distribution of LZ and DZ phenotypes of bulk and c-Myc-GFP$^+$ GC B cells were also unaltered by the inability of the B cells to signal via MyD88 (Supplemental Fig. 3C). The per cell c-Myc-GFP MFI was also similar in WT-Myc-GFP and B-MyD88$^-$Myc-GFP groups (Supplemental Fig. 3D). Thus, there was a non–B cell–intrinsic effect of attaching a TLR9 ligand to NP-CGG on expression of c-Myc-GFP. Moreover, these results suggest that the increased c-Myc transcription signature resulting

Author Manuscript Author Manuscript Author Manuscript Author Manuscript

from TLR9/MyD88 signaling in GC B cells (Fig. 1) may have resulted from a regulatory change in c-Myc transcriptional activity, rather than an increase in c-Myc protein expression.

Dual TLR9 and BCR signaling increases phosphorylation of ribosomal protein S6 in naive B cells and in GC B cells

Next, we examined whether TLR9/MyD88 signaling in purified naive splenic B cells leads to enhanced Akt/mTOR signaling. Initially, purified naive splenic B cells were stimulated in vitro with anti-IgM complex Ags as before, and phosphorylation of mTORC1 targets was assessed by intracellular staining of permeabilized cells with phospho-specific Abs and flow cytometry. Remarkably, phosphorylation of ribosomal protein S6 on residues 235, 236, 240 and 244, known mTORC1 targets detected by Abs specific for phosphorylated residues 235 and 236 [pS6(ser235/236)] or for residues 240 and 244 [pS6(ser240/244)], was almost entirely dependent on CpG stimulation in naive B cells (Fig. 3A, Supplemental Fig. 4A). Anti–IgM-CpG–stimulated WT cells were 90% positive for pS6(ser240/244) at 24 h compared with the 5–15% range seen for WT B cells stimulated with anti–IgM-Non or for B-MyD88^{-} B cells treated with either stimulus (Fig. 3B). The anti–IgM-CpG–stimulated WT B cells showed the highest pS6(ser240/44) MFI, which was 14 times greater than any other group (Fig. 3B). Cell size is in part dependent upon protein content of the cell, and WT B cells stimulated with anti–IgM-CpG also showed the largest increase in cell size forward light scatter compared with the three other groups (Fig. 3B), which is consistent with a role of mTORC1 in enhancing global protein synthesis.

Next, we examined the effect of including a TLR9 ligand attached to NP-CGG on the size of GC B cells and on their pS6 phosphorylation status. GC B cells were substantially larger than naive B cells, as would be expected, but no differences in cell size were evident when comparing B-MyD88^{-} and WT GC at D14 postimmunization with NP-CGG-CpG Ag (Fig. 3C). Additionally, no difference in cell size was evident when only NP-binding GC B cells of these two genotypes were compared (Fig. 3C). Using phospho-flow cytometry, we analyzed pS6(ser240/244) and pS6(ser235/236) in GC B cells. There was an increase in pS6(ser240/244) MFI of WT compared with B-MyD88^{-} GC B cells that was significant ($p = 0.021$) (Fig. 3D). However, we found that WT and B-MyD88^{-} GC B cells exhibited similar MFI staining for pS6(ser235/236) (Supplemental Fig. 4B). When mice were immunized with NP-CGG-CpG versus NP-CGG-Non, we found a 2-fold increase in both pS6(ser240/244) (Fig. 3E) and pS6(ser235/236) in GC B cells (Supplemental Fig. 4C). Interestingly we saw an increase in the pS6 level of non-GC B cells in the NP-CGG-CpG–immunized mice compared with NP-CGG-Non, indicating that another CpG responsive cell type alters the metabolic and inflammatory environment of the lymph node, increasing mTORC1 activity in non-GC B cells in a non–cell-intrinsic manner. Thus, combined CpG-induced TLR signaling and BCR signaling positively regulated mTORC1 signaling robustly in naive B cells, and although all GC B cells had evidence of active mTORC1 signaling, consistent with previous studies (19, 32, 33), TLR9/MyD88 signaling appeared to further increase phosphorylation of the mTORC1 target pS6 by both B cell–intrinsic and –extrinsic mechanisms.

Author Manuscript Author Manuscript Author Manuscript Author Manuscript

Ex vivo stimulation of GC B cells with CpG oligo increases mTORC1 phosphorylation targets and c-Myc induction similarly to CD40 stimulation

To test whether TLR signaling ex vivo in GCB cells would enhance mTORC1 signaling and c-Myc expression in the absence of continued Tfh cell interaction, GC B cells were isolated from immunized Em-BCL2 transgenic mice (to promote their survival during in vitro culture) and stimulated with anti-CD40, anti-IgM, anti-IgM + CpG oligo, or anti-CD40 + anti-IgM for 4 h and fixed before staining for pS6(ser240/244). It was previously reported that both anti-IgM and anti-CD40 signaling are necessary to increase mTORC1 activity and induce c-Myc expression in GC B cells, whereas naive B cells respond to either stimulus individually(34). Similarly, we found that stimulation of naive B cells with anti-IgM and/or anti-CD40 for 4 h led to at least 90% of cells being pS6(ser240/244) positive (Fig. 4A, 4B). Furthermore, CpG stimulation led to 75% of naive cells being pS6(ser240/244) positive, and the addition of anti-IgM increased the response to >95% pS6(ser240/244) positive (Fig. 4A, 4B). In contrast, ex vivo stimulation of Em-BCL2 transgenic GC B cells with anti-IgM alone failed to induce increased phosphorylation of this residue compared with unstimulated GC B cells (Fig. 4A, 4B). Either anti-CD40 or CpG oligo stimulation conditions increased the percentage of pS6(ser240/244)-positive Em-BCL2 GC B cells to comparable levels (50–60%) (Fig. 4A, 4B). These results demonstrate that TLR9 stimulation and CD40 engagement can have similar effects on mTORC1 signaling in GC B cells. Furthermore, stimulation of the BCR via anti-IgM did not increase the response to anti-CD40 or CpG oligo in the Em-BCL2 GC B cells.

Next, we crossed the c-Myc-GFP$^{+/+}$ mice to the Eμ-BCL2 transgenic mice to facilitate examination of c-Myc expression in naive and GC B cells stimulated ex vivo. Naive c-Myc-GFP$^{+/WT}$ B cells and c-Myc-GFP$^{+/WT}$ Eμ-BCL2 GC B cells were stimulated with anti-IgM, anti-CD40, or CpG oligos or combinations thereof. All stimulation conditions increased the expression of c-Myc-GFP substantially in the naive B cells (MFI increased 2.4-fold by anti-IgM, 2.0-fold by anti-CD40, 1.7-fold by CpG, 3.7-fold by anti-IgM + anti-CD40, and 3.8-fold by anti-IgM + CpG, compared with no stimulation), which is congruent with previous studies demon-stratingthat CpG induces c-Myc expression in immature and naive B cells(35,36). Thus, c-Myc induction in naive cells was responsive to each stimulus individually and exhibited an additive response to multiple stimuli. For the Em-BCL2 GC B cells, ex vivo anti-IgM stimulation did not induce c-Myc expression above the unstimulated control (1.1-fold increase in MFI) (Fig. 4C, 4D), similar to what was seen with phosphorylation sites on ribosomal protein S6. Incontrast, stimulation with CpG oligo oranti-CD40induced small but significant increases in c-Myc-GFP expression (MFI increased by 1.3-fold, $p = 0.0007$ and 1.2-fold, $p = 0.0013$, respectively, compared with no stimulation).Addition of anti-IgM may have further increased c-Myc-GFP expression, but it was not statistically significant compared with the individual stimulations. Thus, we did not see a clear synergy between anti-IgM and anti-CD40 stimulation for the induction of c-Myc expression or mTORC1 signaling, in contrast to a previous report (34). As both c-Myc expression and phosphorylation of a key mTORC1 target were increased to similar levels upon stimulation of GC B cells with anti-CD40 or CpG oligo, it is possible that TLR9 signaling in GC B cells could be a partial surrogate for CD40-mediated Tfh cell help. According to this interpretation, more GC B cells would get prosurvival mTORC1 signaling

Author Manuscript Author Manuscript Author Manuscript Author Manuscript

and c-Myc induction in the context of TLR9 signaling in the GC, lowering the need for CD40 stimulation and Tfh cell help. This would increase the number of cells that survive and the pool of GC B cells as a percentage of the B cell population.

DISCUSSION

Previous work established that a TLR ligand attached to a haptenated protein Ag or contained within a virus particle can promote the magnitude and quality of the GC reaction and, moreover, that TLR signaling within the Ag-specific B cell is an important contributor to that enhancement (7, 13). In this study, we used mRNA sequencing and GSEA to identify the intracellular transcriptional programs that were enhanced by coupled Ag and TLR9/MyD88 signaling in GC B cells. Especially enhanced were the transcriptional signatures associated with c-Myc transcriptional activity and mTORC1 signaling. Both of these pathways are central to the control of cell growth and proliferation in many cell types and are critical in B cells for the GC response (17, 32, 33). Interestingly, Tfh cells recognizing Ag presented by GC B cells also stimulate these pathways in the Ag-presenting GC B cell, leading to positive selection of the GC B cells (18, 19, 37). Thus, one potential mechanism by which TLR9/MyD88 signaling may have enhanced c-Myc transcription and mTORC1 signaling is by enhancing interactions of GC B cells with Tfh cells. Alternatively, TLR9/MyD88 signaling in the Ag-specific B cells may have directly increased the transcriptional activities of one or both of these pathways. Consistent with the latter, direct mechanism, we found that ex vivo stimulation of Bcl2-transgenic GC B cells with a TLR9 ligand increased expression of a c-Myc-GFP protein reporter and increased phosphorylation of the mTORC1 target protein ribosomal protein S6, in both cases, similarly to the response induced by anti-CD40, which mimics a key aspect of helper T cell action.

It is likely that several mechanisms contributed to the enhanced c-Myc transcriptional activity seen in Ag-specific GC B cells responding to NP-CGG-CpG immunization. Both naive B cells and Bcl2-transgenic GC B cells cultured ex vivo and stimulated with a TLR9 ligand oligo exhibited increased c-Myc-GFP protein reporter induction, indicating direct TLR9/MyD88 signaling can induce elevated levels of c-Myc protein. Moreover, MyD88 signaling has been shown to stabilize c-Myc protein in intestinal epithelial cells (38). However, the increase in c-Myc-GFP expression in vivo after immunization with the NP-CGG-CpG conjugate was seen not only in WT mice but also in mice in which MyD88 was deleted selectively in B cells, indicating that the observed increase in c-Myc-GFP can also occur by an indirect mechanism, mostly likely by induction following cognate interactions with Ag-specific Tfh cells. This indirect mechanism of promoting c-Myc protein expression in GC B cells could result from TLR9 signaling in other cell types, such as conventional dendritic cells or stromal cells such as follicular dendritic cells. Indeed, previous studies showed that TLR9 signaling in dendritic cells enhanced the number of Tfh cells following immunization with NP-CGG-CpG (13), possibly indicating increased availability of Tfh cell help for GC B cells. Interestingly, c-Myc protein levels were similar in WT and MyD88^{-} GC B cells immunized with NP-CGG-CpG, whereas the c-Myc transcriptional program was stronger in the former mice. The lack of concordance between gene expression data in sorted GC B cells and c-Myc-GFP fluorescent reporter expression indicates that c-Myc–dependent transcription is not necessarily directly proportional to c-Myc protein levels in GC B cells.

Author Manuscript Author Manuscript Author Manuscript Author Manuscript

Therefore, differences in the c-Myc–driven transcriptional signature could be orchestrated through c-Myc phosphorylation, binding partners, or chromatin accessibility (39, 40) programmed in activated B cells by dual BCR/TLR9 signaling that persists into the GC fate. This GC B cell–intrinsic enhancement of c-Myc transcriptional activity would perhaps enhance the effect of Tfh induction of c-Myc protein by making that c-Myc more active and driving higher levels of gene expression, accounting for the transcriptional profiling results.

The increased mTORC1 transcriptional signature identified by GSEA in GC B cells of mice immunized with NP-CGG-CpG was mirrored by increased phosphorylation of ribosomal protein S6, a downstream target of mTORC1. Although the MyD88^{-} GC B cells showed a subtle defect in ribosomal protein S6 phosphorylation in vivo, the remaining observed response in these cells could have been due to CD40 stimulation resulting from cognate interactions with Tfh cells. In addition, we observed that ex vivo stimulation of GC B cells with a TLR9 ligand also induced an increase in phospho-S6 in the GC B cells, indicating that the NP-CGG-CpG likely also directly stimulated this pathway in WT GC B cells. Previous studies have demonstrated MyD88-mediated mTORC1 activation and binding in innate immune cells, and a similar process could occur in GC B cells (41).

Although TLR agonists can promote both T-independent and T-dependent Ab responses, the nature of the Ag and the presence of additional adjuvants can have a major impact on the contribution of TLR signaling to the response. Previous work has shown that the valency of the Ag and its propensity to cross-link the BCR dictate the impact of B cell–intrinsic MyD88-mediated signaling in shaping the GC response. Immunization with monovalent T-dependent Ags (such as OVA) fused to CpG oligo shows no difference in GC B cell numbers or Ab titers between B-MyD88^{-} and WT mice (7, 42), whereas B-MyD88^{-} mice immunized with multivalent VLPs have a profound deficit in the GC response and Ab titers compared with WT mice (7, 14). Furthermore, addition of the lipid adjuvant DOTAP in conjunction with CpG oligo and NP-CGG, forming a multivalent particulate Ag, increased GC B cell and Tfh numbers as well as both high-affinity and low-affinity NP-specific Ab titers when compared with immunization with CpG oligo and NP-CGG in soluble form (15). However, when the same group performed experiments with CpG oligo and NP-CGG complexed with alum, they saw a decrease in high-affinity Ab titers against NP in WT mice compared with B-MyD88^{-} mice (43). Moreover, the inclusion of alum to complex a large murine self-CpG DNA molecule with an amyloid conformed protein (chemically modified human serum albumin) also diminished total GC number and total anti–human serum albumin titers (28). These differences demonstrate that the exact conformation of the protein CpG oligo complex and other adjuvants, specifically alum, can profoundly affect the quality and quantity of the humoral response. The inclusion of alum and its inflammasome-mediated adjuvant activity in monocytes (44, 45) could be a complicating factor in these two experimental settings in which a decrease in the GC response was observed.

Although it is clear that TLR9 signaling in B cells can substantially promote the GC response (13–15), the exact timing of when TLR9-mediated MyD88 signaling influences the GC fate has not been well defined. This signaling event during early B cell activation could provide a selective advantage for initiating the GC or, alternatively, TLR9/MyD88 signaling event in GC cells could directly enhance their ongoing participation in the GC reaction. The

Author Manuscript Author Manuscript Author Manuscript Author Manuscript

enhanced c-Myc and mTORC1 transcriptional programs seen in GC B cells on D14 are certainly consistent with the latter possibility, but these possibilities are not mutually exclusive. In our in vivo and ex vivo stimulation experiments, both naive and GC B cells responded directly to TLR9 stimulation by upregulating mTORC1 signaling and c-Myc protein expression. However, recent studies have demonstrated that MyD88 signaling during the initial activation of naive B cells in the response to nucleic acid-containing VLPs also plays a key role in activated B cell survival, proliferation, and Ag presentation to cognate T cells (23,46). Furthermore, deletion of Myd88 in activated B cells using Aicda-cre had a lesser effect than deletion of Myd88 with Mb1-cre prior to immunization, indicating that TLR/MyD88 signaling during the early phase of the responseis important in the response to CpG-containing VLPs (14). This observation bolsters the idea that dual BCR and TLR9 signaling in naive B cells provides a selective advantage that is maintained days later in the GC response. Thus, the difference in numbers and percentage of GC B cells could be a result of differences in early activation, although our gene expression data indicate that there are persistent MyD88-signaling events that are maintained during the GC, at least through D14.

Both BCR and cosignaling through TLRs and anti-CD40 have been implicated in the metabolic reprogramming of activated B cells. Studies of early activation of B cells in vitro by BCR stimulation, TLR4 stimulation with LPS, or anti-CD40 + IL-4 stimulation to mimic helper T cell action have implicated increased glycolytic flux and increased oxidative phosphorylation as critical metabolic shifts during the initial activation of naive cells and for Ab production in vitro (47, 48). Interestingly, B cells that receive a BCR-mediated signal alone undergo toxic mitochondrial reprogramming, leading to apoptosis unless a secondary signal such as TLR stimulation or CD40-mediated signaling rescues this metabolic dysfunction (23). Thus, activation signals in naive B cells directly reprogram the mitochondria and necessitate cosignaling events for survival; however, the metabolic reprograming that occurs in GC B cells remains largely unknown. As discussed above, it is clear that Tfh cell help induces mTORC1 signaling and c-Myc expression (17–19), two mediators of metabolism and cell cycle regulation. Previous studies have implicated a synergy between BCR stimulation and anti-CD40–mediated Tfh cell help to induce mTORC1 (34), and our ex vivo stimulation data support the idea that cosignaling of BCR and TLR9/MyD88 induce mTORC1. In addition, we found that TLR9/MyD88 signaling in GC B cells enhanced expression of genes involved in oxidative phosphorylation and mitochondrial function (Fig. 1B, Supplemental Fig. 2, Table II).

This work adds to our basic understanding of the molecular pathways within the GC B cell by which TLR recognition promotes their response and has shown that this involves activation of mTORC1 and increased c-Myc transcriptional activity, two critical events also resulting from Ag presentation to Tfh cells. Such understanding may facilitate efforts to improve current vaccines or create new effective vaccines by rational approaches. The tight association of a CpG oligo to a protein Ag is in most circumstances sufficient to promote an increased humoral immunity and could serve as a strategy for vaccination, as can the use of VLPs containing nucleic acid ligands for TLR9 or TLR7. Such immunogens likely mimic to some degree the nature of virus particles and engage an evolutionarily derived mechanism to defend against viral infections. Using endosomal TLR adjuvants to shape the humoral response and provide more GC B cells could be beneficial in antiviral vaccine development.

Author Manuscript Author Manuscript Author Manuscript Author Manuscript

Supplementary Material

Refer to Web version on PubMed Central for supplementary material.

ACKNOWLEDGMENTS

We thank all members of the Ansel Laboratory for discussion; John Gagnon for help with downstream analysis/visualization of the RNA-seq data; Jason Cyster for discussion and guidance on experiments and data interpretation; the University of California, San Francisco functional genomics core, specifically Joshua Pollack, Andrea Barczak, and David Erle, for RNA-seq library generation and sequencing; and the University of California, San Francisco flow cytometry core for access to and maintenance of BD Biosciences instruments.

This work was supported by National Institutes of Health Grants R01HL109102 (to K.M.A.), R21AI117378 (to A.L.D.), and T32AI007334 (to E.J.W.).

Abbreviations used in this article:

B-MyD88^{-}	Mb1-cre^{+} MyD88$^{fl/fl}$
B-MYD88^{-}Myc-GFP	Mb1-cre^{+} MyD88$^{fl/fl}$ Myc-GFP$^{+/+}$
CGG	chicken g globulin
D14	day 14
DZ	dark zone
FDR	false discovery rate
GC	germinal center
GSEA	Gene Set Enrichment Analysis
LZ	light zone
MFI	mean fluorescence intensity
NES	normalized enrichment score
NP	4-hydroxy-3-nitro-phenylacetyl
oligo	deoxyoligonucleotide
pS6(ser235/236)	protein S6 phosphorylated at serine 235/236
pS6(ser240/244)	protein S6 phosphorylated at serine 240/244
RNA-seq	RNA sequencing
Tfh	T follicular helper
VLP	virus-like particle
WT	wild-type

Author Manuscript Author Manuscript Author Manuscript Author Manuscript

REFERENCES

1. Akira S, and Takeda K. 2004 Toll-like receptor signalling. Nat. Rev. Immunol 4: 499–511. [PubMed: 15229469]
2. Blasius AL, and Beutler B. 2010 Intracellular toll-like receptors. Immunity 32: 305–315. [PubMed: 20346772]
3. Iwasaki A, and Medzhitov R. 2004 Toll-like receptor control of the adaptive immune responses. Nat. Immunol 5: 987–995. [PubMed: 15454922]
4. Gavin AL, Hoebe K, Duong B, Ota T, Martin C, Beutler B, and Nemazee D. 2006 Adjuvant-enhanced antibody responses in the absence of toll-like receptor signaling. Science 314: 1936–1938. [PubMed: 17185603]
5. Pasare C, and Medzhitov R. 2005 Control of B-cell responses by Toll-like receptors. Nature 438: 364–368. [PubMed: 16292312]
6. Eckl-Dorna J, and Batista FD. 2009 BCR-mediated uptake of antigen linked to TLR9 ligand stimulates B-cell proliferation and antigen-specific plasma cell formation. Blood 113: 3969–3977. [PubMed: 19144984]
7. Hou B, Saudan P, Ott G, Wheeler ML, Ji M, Kuzmich L,Lee LM, Coffman RL, Bachmann MF, and DeFranco AL. 2011 Selective utilization of Toll-like receptor and MyD88 signaling in B cells for enhancement of the antiviral germinal center response. Immunity 34: 375–384. [PubMed: 21353603]
8. Jegerlehner A, Maurer P, Bessa J, Hinton HJ, Kopf M, and Bachmann MF. 2007 TLR9 signaling in B cells determines class switch recombination to IgG2a. J. Immunol 178: 2415–2420. [PubMed: 17277148]
9. Clingan JM, and Matloubian M. 2013 B Cell-intrinsic TLR7 signaling is required for optimal B cell responses during chronic viral infection. J. Immunol 191: 810–818. [PubMed: 23761632]
10. Chaturvedi A, Dorward D, and Pierce SK. 2008 The B cell receptor governs the subcellular location of Toll-like receptor 9 leading to hyperresponses to DNA-containing antigens. Immunity 28: 799–809. [PubMed: 18513998]
11. O'Neill SK, Veselits ML, Zhang M, Labno C, Cao Y, Finnegan A,Uccellini M, Alegre ML, Cambier JC, and Clark MR. 2009 Endocytic sequestration of the B cell antigen receptor and toll-like receptor 9 in anergic cells. Proc. Natl. Acad. Sci. USA 106: 6262–6267. [PubMed: 19332776]
12. Rawlings DJ, Metzler G, Wray-Dutra M, and Jackson SW. 2017 Altered B cell signalling in autoimmunity. Nat. Rev. Immunol 17: 421–436. [PubMed: 28393923]
13. Rookhuizen DC, and DeFranco AL. 2014 Toll-like receptor 9 signaling acts on multiple elements of the germinal center to enhance antibody responses. Proc. Natl. Acad. Sci. USA 111: E3224–E3233. [PubMed: 25053813]
14. Tian M, Hua Z, Hong S, Zhang Z, Liu C, Lin L, Chen J, Zhang W,Zhou X, Zhang F, et al. 2018 B cell-intrinsic MyD88 signaling promotes initial cell proliferation and differentiation to enhance the germinal center response to a virus-like particle. J. Immunol 200: 937–948. [PubMed: 29282308]
15. Akkaya M, Akkaya B, Sheehan PW, Miozzo P, Pena M, Qi CF,Manzella-Lapeira J, Bolland S, and Pierce SK. 2017 T cell-dependent antigen adjuvanted with DOTAP-CpG-B but not DOTAP-CpG-A induces robust germinal center responses and high affinity antibodies in mice. Eur. J. Immunol 47: 1890–1899. [PubMed: 28762497]
16. Giles JR, Neves AT, Marshak-Rothstein A, and Shlomchik MJ. 2017 Autoreactive helper T cells alleviate the need for intrinsic TLR signaling in autoreactive B cell activation. JCI Insight 2: e90870. [PubMed: 28239656]
17. Calado DP, Sasaki Y, Godinho SA, Pellerin A, Kochert K, Sleckman BP, de Alborán IM, Janz M, Rodig S, and Rajewsky K. 2012 The cell-cycle regulator c-Myc is essential for the formation and maintenance of germinal centers. Nat. Immunol 13: 1092–1100. [PubMed: 23001146]
18. Dominguez-Sola D, Victora GD, Ying CY, Phan RT, Saito M,Nussenzweig MC, and Dalla-Favera R. 2012 The proto-oncogene MYC is required for selection in the germinal center and cyclic reentry. Nat. Immunol 13: 1083–1091. [PubMed: 23001145]

Author Manuscript Author Manuscript Author Manuscript Author Manuscript

19. Ersching J, Efeyan A, Mesin L, Jacobsen JT, Pasqual G,Grabiner BC, Dominguez-Sola D, Sabatini DM, and Victora GD. 2017 Germinal center selection and affinity maturation require dynamic regulation of mTORC1 kinase. Immunity 46: 1045–1058.e6. [PubMed: 28636954]
20. Pua HH, Steiner DF, Patel S, Gonzalez JR, Ortiz-Carpena JF,Kageyama R, Chiou NT, Gallman A, de Kouchkovsky D, Jeker LT, et al. 2016 MicroRNAs 24 and 27 suppress allergic inflammation and target a network of regulators of T helper 2 cell-associated cytokine production. Immunity 44: 821–832. [PubMed: 26850657]
21. Cato MH, Yau IW, and Rickert RC. 2011 Magnetic-based purification of untouched mouse germinal center B cells for ex vivo manipulation and biochemical analysis. Nat. Protoc 6: 953–960. [PubMed: 21720310]
22. Subramanian A, Tamayo P, Mootha VK, Mukherjee S, Ebert BL,Gillette MA, Paulovich A, Pomeroy SL, Golub TR, Lander ES, and Mesirov JP. 2005 Gene set enrichment analysis: a knowledge-based approach for interpreting genome-wide expression profiles. Proc. Natl. Acad. Sci. USA 102: 15545–15550. [PubMed: 16199517]
23. Akkaya M, Traba J, Roesler AS, Miozzo P, Akkaya B, Theall BP,Sohn H, Pena M, Smelkinson M, Kabat J, et al. 2018 Second signals rescue B cells from activation-induced mitochondrial dysfunction and death. Nat. Immunol 19: 871–884. [PubMed: 29988090]
24. Bilanges B, Argonza-Barrett R, Kolesnichenko M, Skinner C, Nair M,Chen M, and Stokoe D. 2007 Tuberous sclerosis complex proteins 1 and 2 control serum-dependent translation in a TOP-dependent and -independent manner. Mol. Cell. Biol 27: 5746–5764. [PubMed: 17562867]
25. Zeller KI, Jegga AG, Aronow BJ, O'Donnell KA, and Dang CV. 2003 An integrated database of genes responsive to the Myc oncogenic transcription factor: identification of direct genomic targets. Genome Biol. 4: R69. [PubMed: 14519204]
26. Raybuck AL, Cho SH, Li J, Rogers MC, Lee K, Williams CL,Shlomchik M, Thomas JW, Chen J, Williams JV, and Boothby MR. 2018 B cell-intrinsic mTORC1 promotes germinal center-defining transcription factor gene expression, somatic hypermutation, and memory B cell generation in humoral immunity. J. Immunol 200: 2627–2639. [PubMed: 29531165]
27. Chiu H, Jackson LV, Oh KI, Mai A, Ronai ZA, Ruggero D, and Fruman DA. 2019 The mTORC1/4E-BP/eIF4E axis promotes antibody class switching in B lymphocytes. J. Immunol 202: 579–590. [PubMed: 30530594]
28. Sindhava VJ, Oropallo MA, Moody K, Naradikian M, Higdon LE,Zhou L, Myles A, Green N, Nundel K, ¨ Stohl W, et al. 2017 A TLR9-dependent checkpoint governs B cell responses to DNA-containing antigens. J. Clin. Invest 127: 1651–1663. [PubMed: 28346226]
29. Huang CY, Bredemeyer AL, Walker LM, Bassing CH, and Sleckman BP. 2008 Dynamic regulation of c-Myc proto-oncogene expression during lymphocyte development revealed by a GFP-c-Myc knock-in mouse. Eur. J. Immunol 38: 342–349. [PubMed: 18196519]
30. Victora GD, Dominguez-Sola D, Holmes AB, Deroubaix S,Dalla-Favera R, and Nussenzweig MC. 2012 Identification of human germinal center light and dark zone cells and their relationship to human B-cell lymphomas. Blood 120: 2240–2248. [PubMed: 22740445]
31. Victora GD, Schwickert TA, Fooksman DR, Kamphorst AO,Meyer-Hermann M, Dustin ML, and Nussenzweig MC. 2010 Germinal center dynamics revealed by multiphoton microscopy with a photoactivatable fluorescent reporter. Cell 143: 592–605. [PubMed: 21074050]
32. Jones DD, Gaudette BT, Wilmore JR, Chernova I, Bortnick A,Weiss BM, and Allman D. 2016 mTOR has distinct functions in generating versus sustaining humoral immunity. J. Clin. Invest 126: 4250–4261. [PubMed: 27760048]
33. Zhang S, Pruitt M, Tran D, Du Bois W, Zhang K, Patel R, Hoover S,Simpson RM, Simmons J, Gary J, et al. 2013 B cell-specific deficiencies in mTOR limit humoral immune responses. J. Immunol 191: 1692–1703. [PubMed: 23858034]
34. Luo W, Weisel F, and Shlomchik MJ. 2018 B cell receptor and CD40 signaling are rewired for synergistic induction of the c-Myc transcription factor in germinal center B cells. Immunity 48: 313–326.e5. [PubMed: 29396161]
35. Arunkumar N, Liu C, Hang H, and Song W. 2013 Toll-like receptor agonists induce apoptosis in mouse B-cell lymphoma cells by altering NF-kB activation. Cell. Mol. Immunol 10: 360–372. [PubMed: 23727784]

Author Manuscript Author Manuscript Author Manuscript Author Manuscript

36. Azulay-Debby H, Edry E, and Melamed D. 2007 CpG DNA stimulates autoreactive immature B cells in the bone marrow. Eur. J. Immunol 37: 1463–1475. [PubMed: 17474151]
37. Mayer CT, Gazumyan A, Kara EE, Gitlin AD, Golijanin J, Viant C,Pai J, Oliveira TY, Wang Q, Escolano A, et al. 2017 The micro-anatomic segregation of selection by apoptosis in the germinal center. Science 358: eaao2602. [PubMed: 28935768]
38. Lee SH, Hu LL, Gonzalez-Navajas J, Seo GS, Shen C, Brick J,Herdman S, Varki N, Corr M, Lee J, and Raz E. 2010 ERK activation drives intestinal tumorigenesis in Apc(min/+) mice. Nat. Med 16: 665–670. [PubMed: 20473309]
39. Conacci-Sorrell M, McFerrin L, and Eisenman RN. 2014 An overview of MYC and its interactome. Cold Spring Harb. Perspect. Med 4: a014357. [PubMed: 24384812]
40. Wang X, Cunningham M, Zhang X, Tokarz S, Laraway B,Troxell M, and Sears RC. 2011 Phosphorylation regulates c-Myc's oncogenic activity in the mammary gland. Cancer Res. 71: 925–936. [PubMed: 21266350]
41. Schmitz F, Heit A, Dreher S, Eisenacher K, Mages J, Haas T, Krug A,Janssen KP, Kirschning CJ, and Wagner H. 2008 Mammalian target of rapamycin (mTOR) orchestrates the defense program of innate immune cells. Eur. J. Immunol 38: 2981–2992. [PubMed: 18924132]
42. DeFranco AL, Rookhuizen DC, and Hou B. 2012 Contribution of Toll-like receptor signaling to germinal center antibody responses. Immunol. Rev 247: 64–72. [PubMed: 22500832]
43. Akkaya M, Akkaya B, Kim AS, Miozzo P, Sohn H, Pena M,Roesler AS, Theall BP, Henke T, Kabat J, et al. 2018 Toll-like receptor 9 antagonizes antibody affinity maturation. Nat. Immunol 19: 255–266. [PubMed: 29476183]
44. MacLeod MK, McKee AS, David A, Wang J, Mason R,Kappler JW, and Marrack P. 2011 Vaccine adjuvants aluminum and monophosphoryl lipid A provide distinct signals to generate protective cytotoxic memory CD8 T cells. Proc. Natl. Acad. Sci. USA 108: 7914–7919. [PubMed: 21518876]
45. McKee AS, and Marrack P. 2017 Old and new adjuvants. Curr. Opin. Immunol 47: 44–51. [PubMed: 28734174]
46. Hong S, Zhang Z, Liu H, Tian M, Zhu X, Zhang Z, Wang W,Zhou X, Zhang F, Ge Q, et al. 2018 B cells are the dominant antigen-presenting cells that activate naive CD4+ T cells upon immunization with a virus-derived nanoparticle antigen. Immunity 49: 695–708.e4. [PubMed: 30291027]
47. Caro-Maldonado A, Wang R, Nichols AG, Kuraoka M, Milasta S,Sun LD, Gavin AL, Abel ED, Kelsoe G, Green DR, and Rathmell JC. 2014 Metabolic reprogramming is required for antibody production that is suppressed in anergic but exaggerated in chronically BAFF-exposed B cells. J. Immunol 192: 3626–3636. [PubMed: 24616478]
48. Waters LR, Ahsan FM, Wolf DM, Shirihai O, and Teitell MA. 2018 Initial B cell activation induces metabolic reprogramming and mitochondrial remodeling. iScience 5: 99–109. [PubMed: 30240649]

Author Manuscript Author Manuscript Author Manuscript Author Manuscript

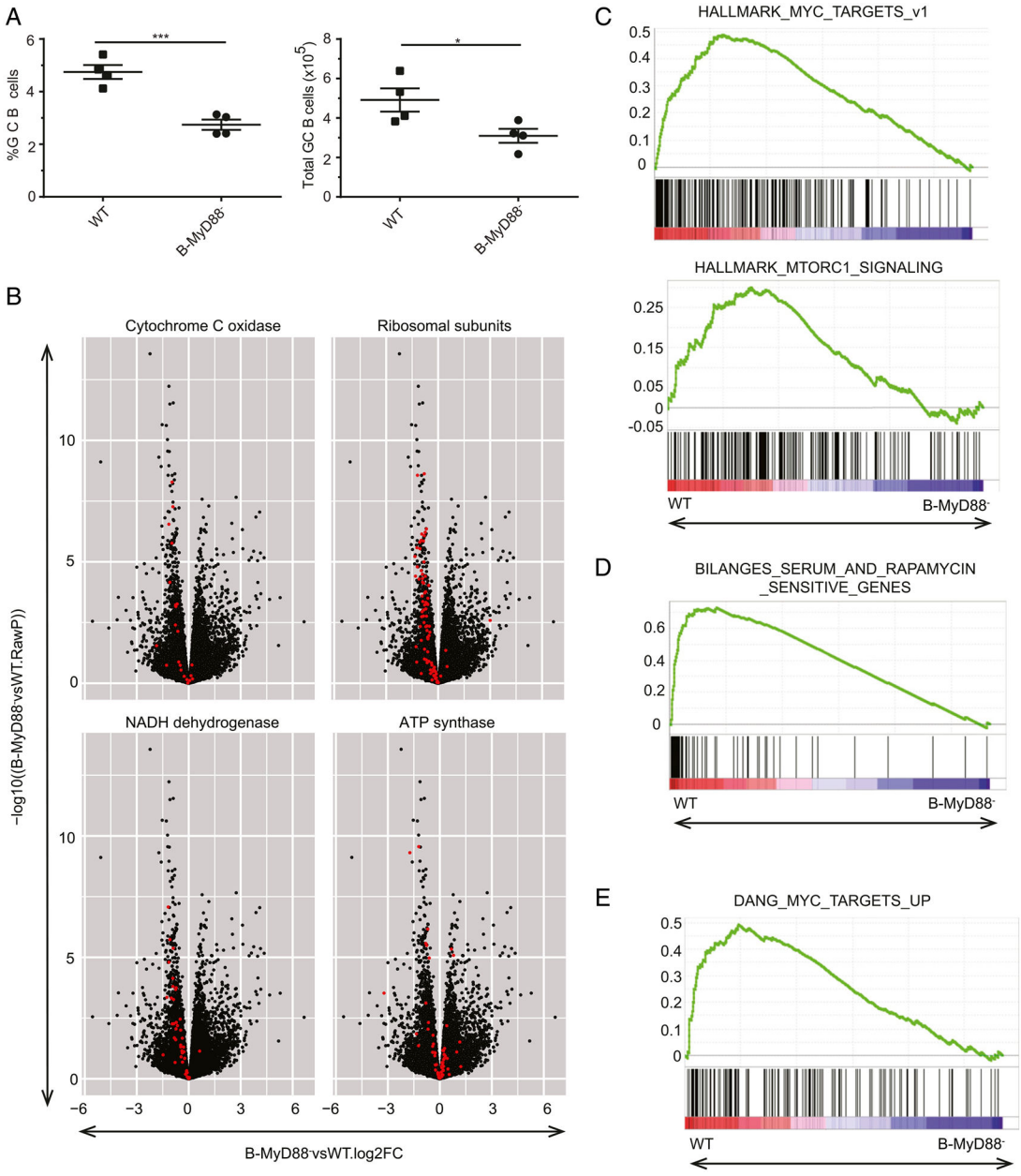

FIGURE 1. mRNA-seq analysis of WT and B-MYD88^{-} NP^{+} GC B cells shows increased c-Myc and mTORC1 gene expression signatures.

(**A**) Enumeration of GC B cell percentages and total cell numbers from draining lymph nodes of WT and B-MYD88^{-} animals at D14 postimmunization. Representative of four independent experiments with at least three mice per group analyzed by a two-tailed Student t test, *$p < 0.05$, ***$p < 0.0005$. (**B**) Volcano plots comparing gene expression fold changes to p values for all genes expressed in at least one sample after DESeq2 analysis. Red dots in each panel indicate genes associated with the given metabolic/synthetic complex listed. (**C**) GSEA plots for hallmark gene sets for mTORC and c-Myc gene signatures enriched in WT transcriptional data. (**D**) GSEA plot from curated gene sets showing enrichment of

rapamycin- and serum-sensitive genes in WT samples. (**E**) GSEA plot from curated gene sets showing enrichment of c-Myc target genes in WT samples.

Author Manuscript Author Manuscript Author Manuscript Author Manuscript

Author Manuscript Author Manuscript Author Manuscript Author Manuscript

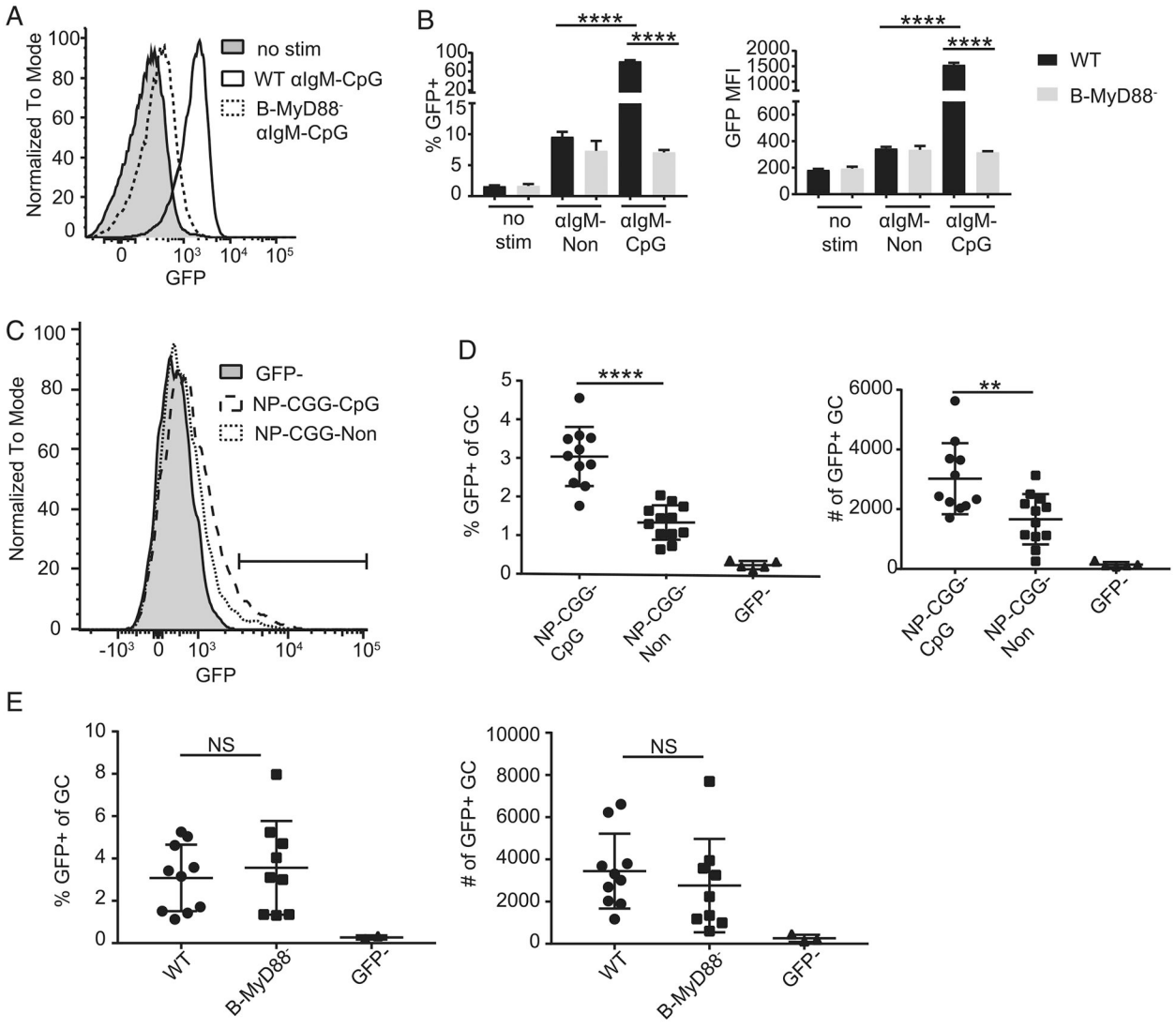

FIGURE 2. Dual BCR/TLR9 signaling positively regulates c-Myc expression in naive and GC B cells.

(**A**) Overlay of representative histograms showing c-Myc-GFP expression in response to anti–IgM-CpG stimulation for 24 h of WT c-Myc-GFP and B-MYD88^{-}c-Myc-GFP naive B cells. (**B**) Enumeration of percent GFP-positive and MFI of cells in (A) (shown is a single experiment representative of three independent experiments). (**C**) Overlay of representative histograms showing GFP fluorescence gating on live, singlet, CD19^{+}, Fas^{+}, IgD^{lo}, and GL7^{+} GC cells of c-Myc-GFP$^{+/+}$ mice immunized with NP-CGG-CpG or NP-CGG-Non D14 postimmunization. (**D**) Enumeration of percent and number of GFP+ GC B cells from NP-CGG-CpG- and NP-CGG-Non-immunized c-Myc-GFP$^{+/+}$ mice (three combined experiments with at least three mice per group). (**E**) Enumeration of percent and number of GFP-positive cells from NP-CGG-CpG–immunized B-MYD88^{-} and WT mice D14 (representative experiment of three independent experiments). $^{**}p < 0.005$, $^{****}p < 0.0001$. NS, $p < 0.05$ by one-way ANOVA and Holm–Sidak multiple comparison test.

Author Manuscript Author Manuscript Author Manuscript Author Manuscript

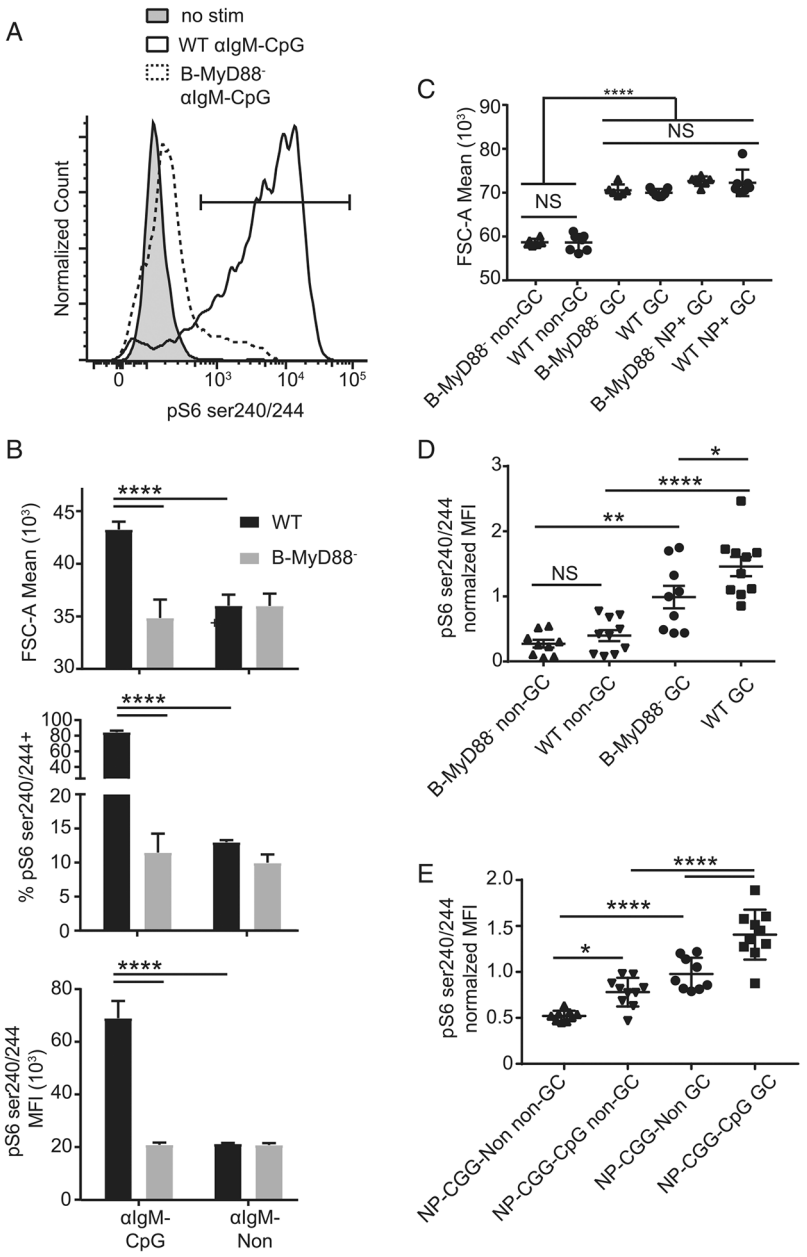

FIGURE 3. Dual BCR/TLR9 signaling positively regulates mTORC1 activity measured by ribosomal protein S6 phosphorylation in naiveand GC B cells.

(**A**) Overlay of representative histograms showing pS6(ser240/244) levels in response to anti–IgM-CpG for 24 h in WT and B-MYD88^{-} naive B cells. (**B**) Enumeration of cell size by forward light scatter (FSC-A), percent pS6(ser240/244)$^{+}$, and MFI of those cells gated positively for pS6(ser240/244) cells for WT and B-MYD88^{-} naive B cells stimulated with anti–IgM-CpG and anti–IgM-Non. (**C**) Enumeration of cell size from D14 NP-CGG-CpG–immunized B-MYD88^{-} and WT non-GC and GC B cells (representative of four independent experiments). (**D**) Phospho-flow MFI of mTORC1 downstream target pS6(ser240/244) D14 NP-CGG-CpG–immunized B-MYD88^{-} and WT B cells normalized to mean of B-MYD88^{-} GC MFI (data are combined from three experiments with at least three mice per group). (**E**)

Author Manuscript Author Manuscript Author Manuscript Author Manuscript

Phospho-flow MFI of mTORC1 downstream target pS6(ser240/244) D14 NP-CGG-CpG- and NP-CGG-Non-immunized mice normalized to mean MFI of NP-CGG-Non MFI (combined from two independent experiments with at least four mice per condition). *$p <$ 0.05, **$p < 0.005$, ****$p < 0.0001$. NS, $p < 0.05$ by one-way ANOVA and Holm–Sidak multiple comparison test.

Author Manuscript Author Manuscript Author Manuscript Author Manuscript

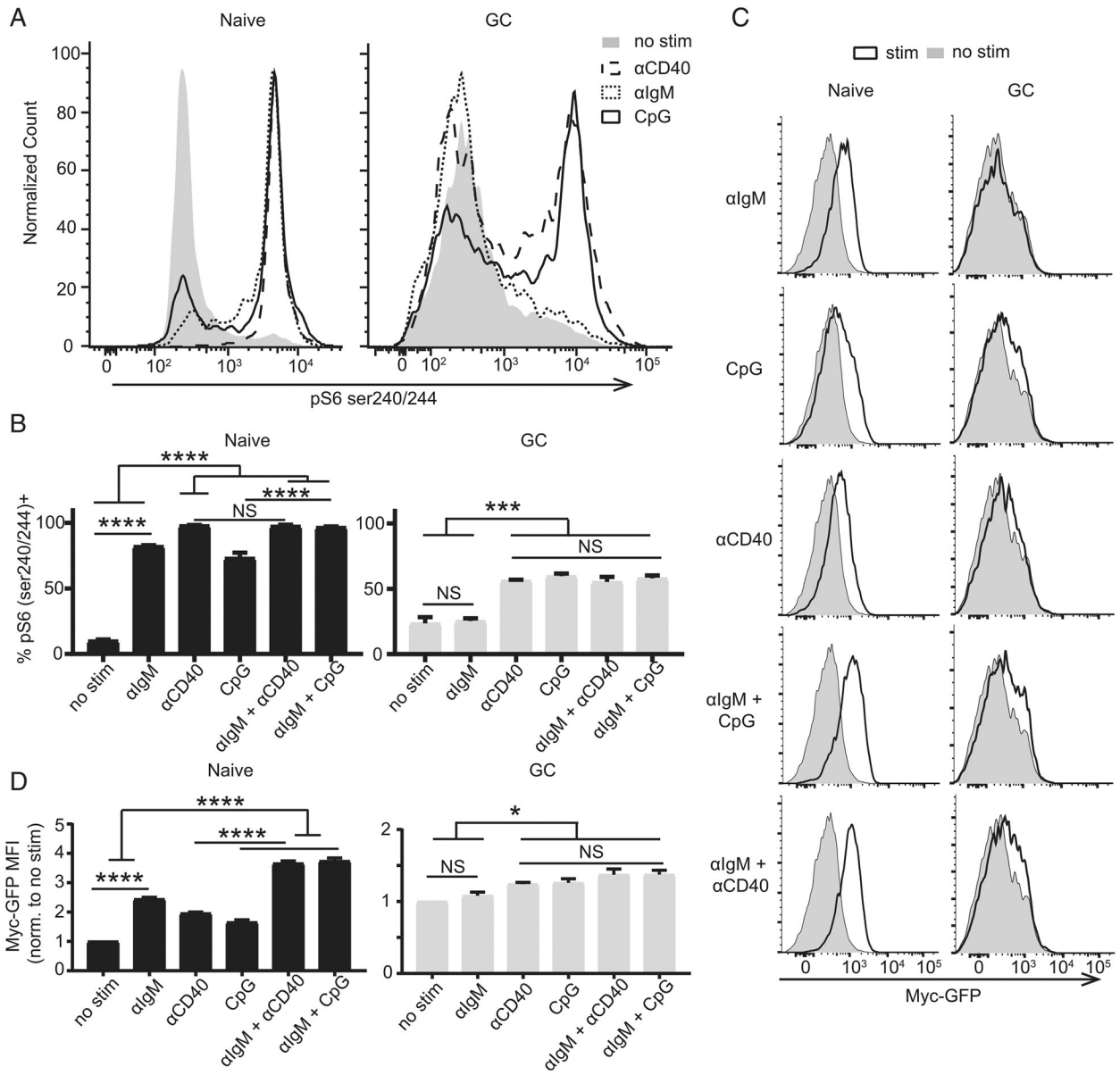

FIGURE 4. CpG stimulation of GC B cells ex vivo increases mTORC1 signaling to similar levels as anti-CD40 stimulation.

(**A**) Representative histograms comparing phospho-flow pS6(ser240/244) staining of 4 h ex vivo–stimulated naive and GC B cells isolated from i.p. NP-CGG alum–immunized mouse spleens at day 12 to D14 (three mice per experiment performed in three separate experiments). (**B**) Enumeration of experiments from (A), showing level of pS6(ser240/244) expression in naive and GC B cells from (A). (**C**) Overlays of c-Myc-GFP expression comparing no stimulation to the respective stimulation in naive and GC B cells after 4 h. (**D**) Enumeration of the relative c-Myc-GFP MFI increase normalized to no stimulation of the samples in (C) (representative of three independent experiments with at least three mice per experiment). *$p < 0.05$, ***$p < 0.001$, ****$p < 0.0001$. NS, $p < 0.05$ by one-way ANOVA and Tukey multiple comparison test.

Author Manuscript

Author Manuscript

Author Manuscript

Author Manuscript

TABLE I.

B cell activation, class switch recombination, and cell fate gene expression

Gene	Log2(KO/WT)	Raw *p* Value	FDR Value
Ighg2c	−0.931278014	2.63×10^{-6}	**0.000742214**
Fas	0.141497226	0.364147352	0.93944051
Cxcr4	0.364550474	0.115060865	0.6353624
Cd86	−0.155604203	0.313582804	0.90908692
Cd80	−0.247780304	0.381587211	0.93944051
Aicda	−0.516289592	0.002956723	0.08882857
Prdm1	−1.091192869	0.003046472	0.08996182
Tir9	0.115035034	0.502823401	0.97633773
Myd88	−1.7156157	2.80×10^{-5}	**0.00412237**
Bcl6	0.39066445	0.000556044	**0.03277441**
Bcl2	−1.081316005	0.000697559	**0.03849734**

Bold indicates FDR < 0.05 and an interpretation of significance. KO, B-MyD88^{-}.

Author Manuscript Author Manuscript Author Manuscript Author Manuscript

TABLE II.

GSEA shows enrichment for mTORC1 and Myc signatures

Name	Size	ES	NES	NOM *p* Value	FDR *q* Value
HALLMARK_OXIDATIVE_PHOSPHORYLATION	186	0.593	2.91	$<1 \times 10^{-4}$	$<1 \times 10^{-4}$
HALLMARK_MYC_TARGETS_V1	191	0.487	2.38	$<1 \times 10^{-4}$	$<1 \times 10^{-4}$
HALLMARK_REACTIVE_OXYGEN_SPECIES_PATHWAY	45	0.517	1.96	$<1 \times 10^{-4}$	4.17×10^{-4}
HALLMARK_PANCREAS_BETA_CELLS	24	0.537	1.76	8.65×10^{-3}	8.19×10^{-3}
HALLMARK_DNA_REPAIR	134	0.360	1.71	$<1 \times 10^{-4}$	1.01×10^{-2}
HALLMARK_E2F_TARGETS	191	0.327	1.60	$<1 \times 10^{-4}$	2.10×10^{-2}
HALLMARK_UNFOLDED_PROTEINRESPONSE	104	0.332	1.49	1.59×10^{-2}	4.61×10^{-2}
HALLMARK_MTORC1_SIGNALING	189	0.299	1.46	4.77×10^{-3}	5.65×10^{-2}
DANG_MYC_TARGETS_UP	129	0.493	2.29	$<1 \times 10^{-4}$	$<1 \times 10^{-4}$
KEGG_RIBOSOME	72	0.819	3.45	$<1 \times 10^{-4}$	$<1 \times 10^{-4}$
BILANGES_SERUM_AND_RAPAMYCIN_SENSITIVE_GENES	59	0.727	2.95	$<1 \times 10^{-4}$	$<1 \times 10^{-4}$

ES, enrichment score; NOM *p* value, nominal *p* value.

Immunohorizons. Author manuscript; available in PMC 2019 September 11.